Genetic Architecture of Mandible Shape in Mice: Effects of Quantitative Trait Loci Analyzed by Geometric Morphometrics

Christian Peter Klingenberg,* Larry J. Leamy,[†] Eric J. Routman[‡] and James M. Cheverud[§]

*Laboratory of Development and Evolution, University Museum of Zoology, Department of Zoology, Cambridge CB2 3EJ, United Kingdom, [†]Department of Biology, University of North Carolina, Charlotte, North Carolina 28223, [‡]Department of Biology, San Francisco State University, San Francisco, California 94132 and [§]Department of Anatomy and Neurobiology, Washington University School of Medicine, Saint Louis, Missouri 63110

ABSTRACT

This study introduces a new multivariate approach for analyzing the effects of quantitative trait loci (QTL) on shape and demonstrates this method for the mouse mandible. We quantified size and shape with the methods of geometric morphometrics, based on Procrustes superimposition of five morphological landmarks recorded on each mandible. Interval mapping for F_2 mice originating from an intercross of the LG/J and SM/J inbred strains revealed 12 QTL for size, 25 QTL for shape, and 5 QTL for left-right asymmetry. Multivariate ordination of QTL effects by principal component analysis identified two recurrent features of shape variation, which involved the positions of the coronoid and angular processes relative to each other and to the rest of the mandible. These patterns are reminiscent of the knockout phenotypes of a number of genes involved in mandible development, although only a few of these are possible candidates for QTL in our study. The variation of shape effects among the QTL showed no evidence of clustering into distinct groups, as would be expected from theories of morphological integration. Further, for most QTL, additive and dominance effects on shape were markedly different, implying overdominance for specific features of shape. We conclude that geometric morphometrics offers a promising new approach to address problems at the interface of evolutionary and developmental genetics.

U NDERSTANDING the evolution of organismal form requires knowledge of the nature of genetic variation in size and shape. This genetic variation can stem from all those genes whose products are involved in the developmental processes that form the structure of interest. One that has long served as a useful model for the development of complex morphological structures is the mouse mandible (*e.g.*, Atchley and Hall 1991; Cheverud *et al.* 1991; Hall 1999, p. 323ff.). Studies using inactivation ("knockout") of specific genes have shown that these disruptions of development can affect different parts of the mandible separately or together (Francis-West *et al.* 1998; Hall 1999, p. 327f.). Moreover, later changes of mandible form through bone remodeling under mechanical load (Herring 1993) are also spatially structured and may rely partly on the same genetic basis, because separate neural crest cell populations migrate to specific locations where they form parts of the mandible as well as the muscle attachments (Köntges and Lumsden 1996). This evidence strongly suggests that the effects of genes on the mandible should be spatially patterned. Thus analysis of gene effects on mandible shape, using quantitative methods,

should advance our understanding of gene action in the development and evolution of form.

Most genetic studies of shape characterize it in terms of the relative sizes of parts and use a set of linear distances for its measurement (*e.g.*, Bailey 1985, 1986; Weber 1990, 1992; Cheverud *et al.* 1997; Leamy *et al.* 1997; Weber *et al.* 1999). A different approach uses a geometric concept of shape, focusing on features such as outlines (Cavicchi *et al.* 1991; Liu *et al.* 1996; Laurie *et al.* 1997; Zeng *et al.* 2000), angles (Whitlock and Fowler 1999), or the geometric configuration of a set of landmark points (Bookstein 1991; Cheverud *et al.* 1991; Dryden and Mardia 1998; Birdsall *et al.* 2000; Gilchrist *et al.* 2000; Zimmerman *et al.* 2000). The analysis of landmark configurations is based on a mathematical framework that describes shape in a complete and nonredundant fashion (for a complete mathematical treatment, see Dryden and Mardia 1998) and also facilitates the graphical inspection of localized morphometric variation. These methods mostly have been used to study phenotypic variation and its possible developmental basis (*e.g.*, Klingenberg and McIntyre 1998; Badyaev and Foresman 2000; Debat *et al.* 2000; Klingenberg and Zaklan 2000), but they are equally suitable for genetic studies (Birdsall *et al.* 2000; Zimmerman *et al.* 2000).

Shape is an inherently multidimensional property. Even for a figure as simple as a triangle, a full description

Corresponding author: Christian Peter Klingenberg, University Museum of Zoology, Downing St., Cambridge CB2 3EJ, United Kingdom. E-mail: cpk24@cam.ac.uk

of shape requires two coordinates to specify the location of a vertex relative to a base line. Shape changes therefore have both a magnitude and a direction in a multidimensional shape space. Traditionally, genetic studies have focused on aspects of shape that can be extracted as scalar measures and then subjected to univariate analyses. These shape measures can be defined *a priori*, for instance, ratios of interlandmark distances (WEBER 1990, 1992; WEBER *et al.* 1999) or angles (WHITLOCK and FOWLER 1999), or they can be chosen as shape features associated with large amounts of phenotypic variation (*e.g.*, principal components from outline data or landmark configurations; LIU *et al.* 1996; LAURIE *et al.* 1997; ZENG *et al.* 2000; ZIMMERMAN *et al.* 2000). This approach is effective for studies focusing specifically on the genetic basis of one particular shape difference, for instance, between two related species, which is inevitably confined to a single direction in shape space. The constraint imposed by the choice of particular shape features is much more serious, however, for studies of variation within populations: the shape effects of segregating genes may or may not coincide with the shape features chosen *a priori*, and there is therefore no guarantee that shape variation is captured completely.

Here we introduce an approach to locate quantitative trait loci (QTL) for shape that is explicitly multivariate throughout every step of the analysis. This procedure simultaneously considers both the magnitude and direction (spatial pattern) of QTL effects and therefore circumvents the choice of a scalar shape measure altogether. This method combines geometric morphometric methods with the multivariate generalization of linkage analysis based on canonical correlation (LEAMY *et al.* 1999, 2000). Rather than constraining the analysis by focusing on a particular shape feature *a priori*, this method examines whether there are differences among marker (or imputed) genotypes in *any* direction of shape space. Therefore, a single analysis can identify QTL affecting all features of shape, reflecting the entire diversity of spatial patterns of gene effects.

This study applies this new approach to characterize the effects of individual QTL producing size or shape changes in the mouse mandible and to examine variation among QTL. We demonstrate our approach with a data set already used in a previous study searching for QTL affecting all 10 pairwise distances among five morphological landmarks (LEAMY *et al.* 1997), which therefore can serve as a basis for direct comparisons of results. Another study in the same mice, based on distance measures derived from a larger set of landmarks, has shown that the effects of some QTL extend over the entire mandible whereas other QTL affect only particular parts (CHEVERUD *et al.* 1997; CHEVERUD 2000). Similar findings have been reported for other parts of the skull (LEAMY *et al.* 1999). These results suggest that groups of QTL differ in the degree to which they affect
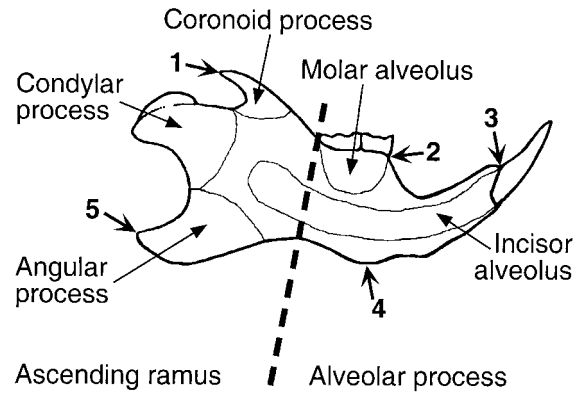
FIGURE 1.—Outline of a mouse mandible showing the five landmark points that were digitized and anatomical regions. The dashed line indicates the approximate boundary between alveolar region and ascending ramus.

various parts of the mandible, just as different gene knockouts produce a variety of phenotypic effects.

We explore this idea systematically by analyzing the geometric patterns of gene effects on mandible shape, and we specifically address the following series of questions that illustrate the new possibilities of this approach: (1) Do the QTL each affect unique aspects of shape, or do they affect a common set of shape features to variable extents? (2) Is there a relation between the geometric patterns of QTL effects and the phenotypes produced by gene knockouts? (3) Are there distinct groups of QTL that have similar effects on mandible shape, perhaps reflecting complexes of genes involved jointly in developmental processes, or are QTL effects continuously distributed? (4) Do additive and dominance effects at each locus correspond to each other, as would be expected if both these effects reflect the developmental function of the respective gene? Our case study demonstrates that the geometric approach for the study of the genetic architecture of shape opens new perspectives on its developmental basis and evolutionary implications.

MATERIALS AND METHODS

Mouse strains and data collection: The mice used in this study were the F_2 progeny of a cross between the Large (LG/J) and Small (SM/J) inbred strains obtained from the Jackson Laboratory (Bar Harbor, ME). These strains originally were selected for large body size (GOODALE 1941) and small body size (MACARTHUR 1944), respectively, although when received by the Jackson Laboratory, both strains were inbred via sibmating (CHAI 1956). A total of 535 F_2 mice were killed at 70 days of age. Subsequently, spleens were removed for DNA extraction, and skeletons were prepared by exposure to dermestid beetles (for additional details, see CHEVERUD *et al.* 1996). Left and right mandible sides were separated at the mandibular symphysis, and the coordinates of five landmarks around the periphery of each mandible were recorded (Figure 1). To assess the precision of measurements, each mandible was digitized three times, yielding three complete sets of coordi-

nates for both left and right sides of the mandibles in each mouse. After removal of outliers and individuals for which mandibles were chipped or broken during the skeletonization or measurement process, the final sample size was 476 mice, including 244 males and 232 females.

DNA was extracted from the spleens of the mice, and a total of 76 polymorphic microsatellite loci were scored in each mouse using PCR amplification (ROUTMAN and CHEVERUD 1994, 1995). These loci mapped in representative areas on the 19 autosomes although none were used on the X chromosome (see ROUTMAN and CHEVERUD 1995). Some loci could not be well resolved on the gels, so the loci varied in their total sample sizes (CHEVERUD *et al.* 1996). Also, one locus, *D10Mit20*, was used only as a dominant marker since the heterozygote could not be distinguished from the SM/J homozygote. The positions of the 76 microsatellite loci were obtained from recombination frequencies with the program Mapmaker 3.0b (LANDER *et al.* 1987; LINCOLN *et al.* 1992). These 76 loci defined a total of 1500 cM (map units in centimorgans) of map distance and included 55 intervals between loci with an average interval length of 27.5 cM (CHEVERUD *et al.* 1996, Table 1 and Figure 1; LEAMY *et al.* 1997, Table 1 and Figure 1).

Morphometric analysis: Our analyses of shape are based on the Procrustes superimposition (BOOKSTEIN 1996a; DRYDEN and MARDIA 1998), as adapted for the study of individual variation and asymmetry (KLINGENBERG and McINTYRE 1998; AUFFRAY *et al.* 1999). These methods define shape as all aspects of the geometric configuration of landmark points except size, location, and orientation. Moreover, because this study includes left and right mandibles, reflection is also ignored, just as a reader wishing to compare the size and shape of his or her left and right hands would put together the palms of both hands. The Procrustes procedure eliminates these features in four steps (KLINGENBERG and McINTYRE 1998):

1. Reflect all left mandibles to their mirror images by changing the signs of the *x* coordinates of all their landmarks.
2. Scale each configuration to unit centroid size. Centroid size is the standard size measure in geometric morphometrics (BOOKSTEIN 1991) and is defined as the square root of the sum of squared distances between each landmark of a configuration and its centroid (the centroid of a configuration is the point whose *x* and *y* coordinates are the means of the *x* and *y* coordinates of all landmarks, respectively).
3. Superimpose the centroids of all configurations by subtracting the mean *x* and *y* coordinates of each configuration from the coordinates of all its landmarks.
4. Rotate the configurations around the centroids to an optimal fit that minimizes the sum of squared distances of the landmarks of each specimen to the corresponding landmarks of the overall mean configuration (generalized least-squares fit).

We carried out separate genetic analyses for overall size, using centroid size, and for shape, using the landmark coordinates of the superimposed configurations. With regard to analyses of shape, two issues should be noted. First, geometric morphometrics defines shape as an inherently multivariate feature. Change in shape is seen as a deformation of the overall configuration of landmarks, and it is therefore difficult to single out changes in particular landmarks. Notably, it is not possible to calculate genetic parameters in univariate analyses for individual landmark coordinates—the coordinates are meaningful only as part of the entire multivariate configuration, as each coordinate is the result of the overall Procrustes fit of the complete configurations.

Second, the elimination of size, position (*x* and *y* coordinates), and orientation of specimens eliminates four degrees of freedom. Therefore, the number of dimensions of the re-

sulting shape space is $2k - 4$ (where k is the number of landmarks), although there are $2k$ coordinates for each superimposed configuration. As a consequence, covariance matrices of the coordinate data are not of full rank, and the degrees of freedom for some statistical tests need to be adjusted. A way to avoid the resulting difficulties is to omit, *after* the Procrustes superimposition of the *complete* configurations, the coordinates of any two landmarks from statistical procedures that involve inversion of the covariance matrix of shape variables (BOOKSTEIN 1996b, p. 140). In our study, we therefore omitted two of the five landmarks of Procrustes-superimposed configurations canonical correlation analysis. Because the remaining six coordinates retain the full information on the shape of the configuration of all five landmarks (which is contained in $2k - 4 = 6$ of the total $2k = 10$ coordinates), this maneuver produces identical statistical results regardless of which two landmarks are omitted.

Sources of variation: Before the genetic analyses, we corrected centroid size and the shape coordinates for the effects of sex, dam, experimental block, and litter size (see CHEVERUD *et al.* 1996, 1997; LEAMY *et al.* 1999). These corrections reduced the total sum of squares for centroid size only by 10.0% and that for shape by 8.3%, but they eliminated extraneous variance due to environmental factors from the genetic analyses. To partition phenotypic variation into among-individuals, within-individuals, and measurement error components, we used the two-way ANOVA design customary for the study of left-right asymmetry of size measurements (LEAMY 1984; PALMER and STROBECK 1986; PALMER 1994), which also has been adapted for shape (KLINGENBERG and McINTYRE 1998). In these ANOVAs, the main effect of individuals stands for individual variation in size or shape. The main effect of body side indicates directional asymmetry, whereas the side × individual interaction provides a measure of fluctuating asymmetry. Finally, the residual variance component among replicate measurements quantifies measurement error. Whereas the ANOVAs for centroid size calculate sums of squares in the usual manner (LEAMY 1984; PALMER and STROBECK 1986; PALMER 1994), the Procrustes ANOVAs for shape are calculated by computing sums of squares for all coordinates and then summing up across landmarks and *x* and *y* coordinates (KLINGENBERG and McINTYRE 1998). In the Procrustes ANOVAs for shape, the usual degrees of freedom are multiplied by the shape dimension ($2k - 4 = 6$ in our study).

Asymmetry measures: Although directional and fluctuating asymmetry are properties of samples or populations (*e.g.*, PALMER and STROBECK 1986), genetic studies require measures for each individual. Such studies (*e.g.*, LEAMY *et al.* 1997) have distinguished two aspects of left-right asymmetry that can be measured for individuals: signed and unsigned asymmetry. Signed asymmetry includes information about the direction of the asymmetry (*e.g.*, left-handed *vs.* right-handed), and genetic variation for signed asymmetry is required for evolutionary change in directional asymmetry (the population mean of signed asymmetry). In contrast, unsigned asymmetry accounts for only the magnitude of the difference between body sides, but not its direction. Fluctuating asymmetry is the mean level of unsigned asymmetry in populations and is often interpreted as a measure of developmental stability (*e.g.*, PALMER 1994). We carried out analyses for both signed and unsigned asymmetry of centroid size and of shape. These asymmetry values were corrected for the average (directional) asymmetry in the sample. Strictly speaking, therefore, we analyzed the signed and unsigned deviations from the mean left-right asymmetry in the sample, which corresponds to using the side × individual interaction in the ANOVA model. These corrected values for signed and unsigned asymmetry, both for centroid size and shape, were entered into the QTL analyses.

Defining unsigned left-right differences in the multivariate context of shape analysis presents another difficulty. It is not possible simply to change all negative signs of individual coordinate differences, because that would constrain the left-right differences of every landmark to point in an anterior and dorsal direction (in the view of Figures 2–4) and thus break up the associations between landmarks. To leave these associations intact, it was necessary to divide the space of possible shape changes into two equal parts (corresponding to "positive" and "negative" left-right differences) and to change the signs of all coordinate differences for all individuals in one of the parts. As a criterion for such a partition, we used the sign of the inner product between the vector of left-right differences of each individual and that of the first specimen in the data set. This computation of "unsigned asymmetry" of shape eliminated the directional component, but left the multivariate relations between landmarks intact.

Interval mapping: QTL analyses were carried out for the left-right means of centroid size and shape, as well as for signed and unsigned asymmetry of centroid size and shape, using the interval mapping method described by Haley and Knott (1992; see also Lynch and Walsh 1998, p. 453ff.). At the locations of molecular markers, additive genotypic deviations were set to -1, 0, and $+1$ and dominance genotypic deviations to 0, $+1$, and 0, respectively, for SM/J homozygotes, heterozygotes, and LG/J homozygotes. For locations between flanking microsatellite markers, in steps of 2 cM, additive and dominance genetic deviations were imputed using recombination frequencies calculated with the program Mapmaker 3.0 (Lincoln *et al.* 1992) and the formulas in Haley and Knott (1992, Table 1). Conditioning markers located on chromosomes other than the one being analyzed were not used as partialing variables to account for potential effects of background genes and other QTL (Jansen 1993; Zeng 1994), because a number of markers were missing and in some cases this would have reduced the sample size considerably.

The QTL analyses of size used the regression method Haley and Knott (1992). Three separate analyses were run for size (in parentheses, the abbreviations used to designate QTL): one each for the left-right average of centroid size (C), for signed asymmetry of centroid size (CS), and for unsigned asymmetry of centroid size (CU).

For shape, multivariate QTL analyses were carried out using canonical correlation to relate shape variables to genotypic deviations (Leamy *et al.* 1999, 2000). The shape variables were the first six coordinates after Procrustes superimposition of the complete configurations (omitting four coordinates to obtain the appropriate dimensionality, see above). At each position 2 cM apart on a given chromosome, canonical correlation analysis generated a pair of new variables, as linear combinations of the genotypic deviations and the shape variables, whose correlations were maximal. Three separate analyses were run for shape: one each for left-right average of shape (SH), for signed shape asymmetry (SS), and for unsigned shape asymmetry (SU).

LOD scores for the presence of a QTL were computed for each 2-cM interval on each chromosome in the canonical correlation runs from the probabilities associated with the *F* approximations to Rao's statistic (Leamy *et al.* 1999, 2000). If the highest LOD score for a given chromosome exceeded the appropriate threshold value, a QTL was considered to be present at the position of that LOD score. The threshold values used for determining the presence of QTL were obtained by a permutation procedure (Churchill and Doerge 1994) done separately for each chromosome and in separate analyses for centroid size and for shape, as well as the respective asymmetries. For each of 1000 permutation runs, the size or shape values for each individual mouse were randomly permuted,

and LOD scores were computed from canonical correlations of these reshuffled values with the imputed genotypic deviations in steps of 2 cM along the chromosome. The 50th and 10th highest LOD scores generated from these 1000 runs provided the 5 and 1% threshold values for each chromosome (denoted "chromosomewise" thresholds below). To compute threshold values for the whole genome, the maximum LOD score across all 19 chromosomes was identified for each of the 1000 permutation runs, and the 50th and 10th highest of these values were used as the genomewide thresholds.

Approximate confidence intervals for each QTL were established according to the one-LOD rule (Lynch and Walsh 1998, p. 448f.), that is, the intervals on either side of the QTL location where there was a drop in the LOD score of 1.0 from the maximum value. QTL positions and confidence intervals were expressed both as distances from the nearest proximal marker and also as distances from the centromere, using the distance from the centromere to the most proximal marker given in the Mouse Genome Database (2000).

Once a QTL was found on a given chromosome, tests were conducted for the presence of two QTL on that chromosome. This was done as described above, but using the imputed genotypic deviations at all possible *pairs* of locations. Bartlett's *V*-statistic (Green 1978), distributed as χ^2 with 4 d.f. for the analyses of size and with 24 d.f. for shape, was computed for each run, and the highest such value generated was compared with its counterpart from the one-QTL run (distributed as χ^2 with 2 d.f. for analyses of centroid size and 12 d.f. for analyses of shape). If the difference between these values exceeded the critical χ^2 value for 2 d.f. (centroid size) or for 12 d.f. (shape), the improvement in fit was considered significant and it was concluded that two QTL were present on that chromosome at the locations indicated by the highest chi-square value. Confidence intervals around both QTL were determined as before, but using LOD scores generated from new canonical correlation runs that partialed out the effect of one QTL and fit a one-QTL model for the other QTL (Leamy *et al.* 1999).

QTL effects: For univariate analyses, the additive genotypic value *a* is defined as one-half the difference between the values for the two homozygotes, whereas the dominance genotypic value *d* is defined as the difference between the average of the two homozygous values and the heterozygous value (Falconer and Mackay 1996). For analyses of shape, additive and dominance effects can be characterized in the same manner by **a** and **d** vectors, respectively. Note that whereas the *a* and *d* values for size are scalars, the **a** and **d** vectors for shape have both a magnitude and direction, reflecting the spatial pattern of additive and dominance effects on shape.

After QTL positions were determined for each chromosome, we carried out multiple regressions of centroid size on the additive and dominance genotypic deviations for the QTL on that chromosome. The regression coefficients for the additive and dominance genotypic deviations, respectively, provided estimates of the *a* and *d* values for size. Similarly, the **a** and **d** vectors for shape were calculated as the vectors of regression coefficients in multivariate regressions of shape (all 10 Procrustes coordinates) on the same additive and dominance genotypic deviations.

While the QTL effects on centroid size (left-right mean as well as asymmetry) can be characterized as *a* and *d* values presented in tabular form, this sort of display is not feasible for the inherently multidimensional shape results. To quantify the magnitude of QTL effects, we tabulated the lengths of additive and dominance vectors in units of Procrustes distance (computed as $\|\mathbf{a}\| = (\mathbf{a'a})^{0.5}$, $\|\mathbf{d}\| = (\mathbf{d'd})^{0.5}$). To visualize the spatial pattern of additive and dominance effects of each QTL for these characters, we graphed the corresponding shape

changes as landmark shifts and as deformations of the outline of a mouse mandible using the method of thin-plate splines (Bookstein 1991; Dryden and Mardia 1998, chapter 10). The outline deformations are meant as visual aids depicting the QTL effects as shape changes in the anatomical context of the whole mandible, but the reader should bear in mind that the graphs rely entirely on the information from the five landmarks. Therefore, the diagrams need to be interpreted with caution in parts of the mandible without nearby landmarks. Because the QTL effects were very subtle, we amplified them by a factor of 25 in all these diagrams to make them more easily visible.

Multivariate analyses of QTL effects: We examined the distribution of QTL effects in the shape space, asking specifically whether QTL effects were clustered in distinct groups and to which extent variation was concentrated in one or just a few dimensions. To identify the dominant patterns of QTL effects and to display the variation among QTL graphically, we used a multivariate ordination by principal component analysis (*e.g.*, Jolliffe 1986). These principal component analyses used the covariance matrix of the **a** and **d** vectors (see also Dryden and Mardia 1998; Klingenberg and McIntyre 1998).

To establish whether there were distinct groups of QTL with regard to their effects on shape, for instance, affecting different parts of the mandible (*e.g.*, Cheverud *et al.* 1997), we searched for clusters in the multivariate distributions of **a** and **d** vectors. To test statistically for clusters of QTL, we used *k*-means clustering (*e.g.*, Krzanowski and Marriott 1995, p. 80) in combination with a parametric bootstrap procedure (Efron and Tibshirani 1993). *k*-means clustering is a nonhierarchical clustering method that searches for the partition of a sample (here, the **a** or **d** vectors of the QTL) into a given number (g) of groups so that the within-group sum of squares is minimal. We considered three possibilities (*cf.* Figure 1; after Cheverud *et al.* 1997): a homogeneous distribution of QTL effects (the null hypothesis, $g = 1$), two groups of QTL affecting either the anterior or posterior portions of the mandible ($g = 2$), or three groups affecting the anterior, posterior, or both portions simultaneously ($g = 3$). We defined the test statistic as the ratio of the within-cluster sum of squares for the two- or three-cluster fits to the total sum of squares (a low value of this measure indicates the improvement of fit for $g = 2$ or $g = 3$ over the null hypothesis with $g = 1$, thus providing evidence for clusters). For the parametric bootstrap test, we simulated the null hypothesis of homogeneous distribution using a multivariate normal distribution with variances equal to the eigenvalues in the original sample. In each of 10,000 simulation runs, the *k*-means clustering was used on a simulated data set corresponding to the number of QTL, and the P value was computed as the proportion of simulations in which the test statistic was lower than that for the corresponding level of g in the original sample.

The correspondence over all QTL between the **a** and **d** vectors for the left-right average of shape was assessed using a permutation test (Edgington 1995). Before the test, we multiplied the **d** vector by -1 if the inner product of the **a** and **d** vectors was negative for that QTL ($\mathbf{a'd} < 0$). The purpose of this step was to eliminate the direction of dominance (*i.e.*, whether the allele of the LG/J or SM/J strain was dominant) because it was not relevant for the comparison of additive and dominance effects on shape. As the test statistic, measuring the magnitude of covariation, we computed the sum of squared covariances between **a** and **d** vectors. For each of 10,000 permutation runs, the **d** vectors were randomly reshuffled among QTL, and the sum of squared covariances was computed and compared to the original value.

Comparisons with previous analyses: We compared our re-sults to two published studies of QTL affecting mandibular morphology in the same mice (Cheverud *et al.* 1997; Leamy *et al.* 1997). Leamy *et al.* (1997, Appendix) present univariate QTL data for all 10 pairwise distances among the same five landmarks as the present study. Cheverud *et al.* (1997) used a more extensive set of landmarks and conducted QTL analyses for 21 pairwise distances. Both studies combined QTL affecting different distances, but located close to each other on the same chromosome, as single loci after univariate analyses. Because of this "aggregate" nature of QTL and the differences in analytic techniques used, formal tests of the similarity of the distribution of QTL through the genome are not feasible (but see Cheverud 2000). We present a tabular comparison of the QTL locations and the affected parts of the mandible.

RESULTS

Sources of variation in size and shape: Variation among individual mice contributes by far the biggest share of the total variation in centroid size, but also more than half of the total shape variation (Table 1). Differences in centroid size and in shape between the left and right mandibles are also highly significant, indicating that directional asymmetry (DA) is present, even though it is fairly subtle (*e.g.*, for centroid size the left and right means are 10.23 and 10.15 mm, respectively). The variance components of the individuals $\times$ sides interaction, representing fluctuating asymmetry (FA), are somewhat greater than the corresponding DA components for both size and shape. The individuals $\times$ sides interaction is highly significant, and its variance component exceeds that of the error severalfold for both centroid size and shape. This indicates that measurement error is not a serious problem for the study of FA in this data set.

QTL for centroid size: The search for QTL affecting the left-right means of centroid size revealed 12 QTL on 11 autosomes (Table 2). Chromosome 11 carries 2 of these significant QTL. The LOD scores for all these QTL except 1 (QTL-C7.1) exceed the 1% chromosomewise threshold values, and 10 of the 12 exceed the 5% genomewide threshold value of 3.254. The centromeric distance for QTL-C2.1 could not be determined because recombination between *D2Mit1* and *D2Mit17* was very near 50% (Cheverud *et al.* 1996). Confidence intervals for these QTL vary from 8 cM (QTL-C17.1) to 84 cM (QTL-C7.1), averaging 36 cM (but note that this average is an underestimate, because all but four of the confidence intervals are delimited by an extreme marker).

The proportion of the total variation in left-right means of centroid size for which the QTL account averages 5.1% and ranges from 2.2 to 8.8% (Table 2). The additive genotypic (*a*) values for all of these QTL are highly significant and average 0.078 mm, which is small relative to the mean centroid size of 10.18 mm (standard deviation = 0.30 mm). All *a* values have positive signs, indicating that the alleles from the Large strain consistently increase the overall size of the mandible. The

TABLE 1

Analysis of variance for centroid size and shape

Source	Sum of squares	d.f.	Mean square	Variance component	% variance
Centroid size					
Individuals (*I*)	216.263	474	0.456**	744.59	93.48
Sides (*S*)	5.253	1	5.253**		
I × *S*	6.744	475	0.0142**	45.78	5.75
Error	1.142	1874	0.000609	6.09	0.77
Shape					
Individuals (*I*)	1.413	2844	0.000496**	66.06	64.20
Sides (*S*)	0.181	6	0.0301**		
I × *S*	0.286	2850	0.000100**	31.79	30.88
Error	0.057	11244	5.06×10^{-6}	5.06	4.92

The analyses for centroid size use the conventional two-factor ANOVA (LEAMY 1984; PALMER and STROBECK 1986), while the analyses of shape use the extension using the Procrustes method (KLINGENBERG and McINTYRE 1998). Sums of squares, mean squares, and variance components are in square millimeters for centroid size (variance components $\times 10^4$) and in dimensionless Procrustes units for shape (variance components $\times 10^6$). The percentage contributions (% variance) of each variance component to the total variance also are given. **$P < 0.01$.

absolute *d* values are substantially smaller than the *a* values (the average of the absolute *d*/*a* ratios is 0.40) and most are not significant statistically, suggesting that the action of the QTL for left-right means of centroid size is predominantly additive in nature. There is one QTL (QTL-C4.1), however, where the *d* value is statistically significant and exceeds the *a* value (*i.e.*, overdominance).

Only two QTL, with questionable statistical significance, appear to affect signed asymmetry of centroid size (Table 2). One of these, on chromosome 10, is located near QTL-C10.1 affecting the left-right mean of centroid size, whereas the other, on chromosome 11, is located between two QTL affecting the left-right means. The LOD scores for both of these putative QTL are low, only slightly exceeding the 5% chromosomewise threshold values and well below the 5% genomewide threshold value of 3.365. These two QTL show statistically significant *a*, but not *d* values (Table 2), although the *a* values and percentages of variation contributed are much lower than the comparable values for the QTL for left-right means.

Only a single QTL for unsigned asymmetry of centroid size reached chromosomewise significance, but also had a LOD score below the 5% genomewide threshold value (3.400), thus making it doubtful statistically (Table 2). Its *a* value is comparable to those of the two QTL for signed asymmetry of centroid size, but in addition it also displays marked underdominance.

QTL for shape: The left-right means of shape are affected by 25 separate QTL on 16 of the 19 chromosomes (Table 3). Eight chromosomes carry 2 QTL each. LOD scores exceed the 1% chromosomewise threshold level for 19 of these 25 QTL, and the 5% genomewide threshold value of 3.408 for 20 QTL. Their confidence

intervals average 28 cM (but note, again, that this is an underestimate because many confidence intervals are truncated at the positions of extreme markers).

Only one QTL was found to affect signed asymmetry of shape (Table 3). It is located on chromosome 15, near QTL for centroid size and shape, and its LOD score exceeds both the 1% chromosomewise threshold value for this chromosome and the 5% genomewide threshold value of 3.284 for signed shape asymmetry. The analyses for unsigned asymmetry of shape suggested another QTL, on chromosome 12, which shows chromosomewise significance, but is associated with a LOD score less than the 5% genomewide threshold value (3.160). Therefore, there is good support for a QTL affecting signed asymmetry of shape, whereas the evidence for the QTL affecting unsigned asymmetry is merely suggestive.

Because shape is inherently multidimensional, QTL effects on shape need to be considered in terms of both their magnitude and spatial patterning. The magnitude of additive and dominance effects of the 25 significant QTL for the left-right means of shape vary: the lengths of the **a** and **d** vectors vary about 4-fold, although all of them are fairly small (Table 3; Figure 2—recall that the diagrams show the effects amplified 25-fold). For most of these QTL, the additive effects are greater than the dominance effects, but the difference is smaller than that for centroid size. The average ratio of dominance to additive effects ($\|\mathbf{d}\|/\|\mathbf{a}\|$) is 0.85, and there are only 5 QTL where this ratio is less than 0.5 (and none less than 1/3). Moreover, for 6 QTL the magnitudes of dominance effects exceed the additive effects, although the dominance effect is statistically significant in only four of these cases. Altogether, dominance appears to play a greater role for shape than for centroid size.

TABLE 2

QTL analysis for centroid size

QTL	LOD	Proximal marker	Marker distance	Centromere distance	Marker C.I.	Centromere C.I.	%	a	S.E. a	d	S.E. d
					Left-right means						
QTL-C2.1	2.80**	D2Mit28	10	—	D2Mit17+2–D2Mit22+0^{end}	—	2.90	0.072**	0.0205	−0.026	0.0335
QTL-C3.1	3.91**	D3Mit22	6	57	D3Mit3+0–D3Mit22+16	27–61	3.76	0.077**	0.0190	0.044	0.0300
QTL-C4.1	3.51**	D4Mit17	0	38	D4Mit2+10–D4Mit17+4	18–42	3.38	0.048**	0.0169	0.072**	0.0240
QTL-C6.1	3.71**	D6Nds5	14	86	D6Mit9+14–D6Mit15+0^{end}	70–100	3.58	0.078**	0.0193	0.032	0.0339
QTL-C7.1	2.22*	D7Mit21	30	31	D7Mit21+0^{end}–D7Mit9+4	1–85	2.15	0.072**	0.0228	0.024	0.0474
QTL-C10.1	6.83**	D10Mit10	6	79	D10Mit20+10–D10Mit10+14	63–87	6.57	0.115**	0.0202	0.013	0.0291
QTL-C11.1	7.08**	D11Mit64	0	47	D11Mit62+16–D11Mit64+8	17–55	8.78	0.069**	0.0178	−0.001	0.0238
QTL-C11.2		D11Mit14	12	91	D11Mit15+10–D11Mit48+0^{end}	67–109		0.077**	0.0219	−0.011	0.0350
QTL-C13.1	4.09**	D13Mit1	20	27	D13Mit1+0^{end}–D13Mit1+38	7–45	3.93	0.100**	0.0229	0.012	0.0461
QTL-C14.1	4.87**	D14Mit5	8	54	D14Nds1+22–D14Mit7+0^{end}	24–64	4.66	0.084**	0.0181	0.038	0.0292
QTL-C15.1	4.01**	D15Mit5	26	55	D15Mit5+12–D15Mit2+8	41–67	3.86	0.079**	0.0186	0.027	0.0281
QTL-C17.1	3.06**	D17Mit46	0	11	D17Mit46+0^{end}–D17Mit46+8	11–19	3.17	0.071**	0.0193	−0.028	0.0253
					Signed asymmetry						
QTL-CS10.1	2.18*	D10Mit20	18	71	D10Mit20+2–D10Mit10+10	55–83	2.11	−0.022**	0.0069	−0.006	0.0097
QTL-CS11.1	2.25*	D11Mit15	14	71	D11Mit64+4–D11Mit48+0^{end}	51–109	2.24	0.019**	0.0068	0.018	0.0111
					Unsigned asymmetry						
QTL-CU5.1	2.35*	D5Mit61	0	30	D5Mit47+22–D5Mit61+32	26–62	2.38	0.018**	0.0089	−0.044**	0.0165

Tabled values are LOD scores, locations (as map distances from the nearest proximal marker and from the centromere), and their confidence intervals (C.I.), the percentage of variation accounted for (%), and additive (a) and dominance (d) genotypic values with their associated standard errors. LOD scores and percentage of variation are indicated per chromosome (*i.e.,* QTL on the same chromosome are combined). The superscript "end" denotes a confidence interval truncated at the position of an extreme marker. $*P < 0.05$; $**P < 0.01$.

TABLE 3

QTL analysis for shape

QTL	LOD	Proximal marker	Marker distance	Centromere distance	Marker C.I.	Centromere C.I.	Additive magnitude $\|\mathbf{a}\|$	Dominance magnitude $\|\mathbf{d}\|$
				Left-right means				
QTL-SH1.1	3.58*	D1Mit20	34	54	D1Mit20+18– D1Mit7+6	38–62	0.00242**	0.00163
QTL-SH1.2		D1Mit14	12	106	D1Mit11+8– D1Mit14+26	78–120	0.00308**	0.00172
QTL-SH2.1	5.62**	D2Mit17	2	—	D2Mit17+0$^{\text{end}}$_ D2Mit28+0	—	0.00387**	0.00237
QTL-SH3.1	4.25**	D3Mit3	10	41	D3Mit3+10– D3Mit22+8	37–53	0.00414**	0.00286*
QTL-SH4.1	4.13**	D4Mit17	2	40	D4Mit2+20– D4Mit17+8	28–46	0.00325**	0.00494*
QTL-SH5.1	2.53*	D5Mit61	28	58	D5Mit61+6– D5Mit6+8	37–105	0.00426**	0.00891*
QTL-SH6.1	6.15**	D6Mit1	0	4	D6Mit1+0$^{\text{end}}$_ D6Mit1+12	4–16	0.00401**	0.00251*
QTL-SH6.2		D6Nds5	14	86	D6Nds5+2– D6Nds5+26	74–98	0.00476**	0.00285
QTL-SH7.1	16.49**	D7Mit21	36	37	D7Mit21+12– D7Nds1+12	13–65	0.00512**	0.00425
QTL-SH7.2		D7Nds1	12	65	D7Nds1+8– D7Mit17+10	61–77	0.00653**	0.00224
QTL-SH9.1	6.06**	D9Mit4	0	30	D9Mit2+0$^{\text{end}}$_ D9Mit4+8	16–38	0.00263**	0.00220
QTL-SH9.2		D9Mit8	34	78	D9Mit8+10– D9Mit19+0$^{\text{end}}$	54–88	0.00274	0.00425*
QTL-SH10.1	6.96**	D10Mit2	20	29	D10Mit2+0$^{\text{end}}$_ D10Mit2+32	9–41	0.00618**	0.00402
QTL-SH10.2		D10Mit20	18	71	D10Mit20+12– D10Mit10+2	65–75	0.00672**	0.00256
QTL-SH11.1	11.87**	D11Mit62	22	23	D11Mit62+12– D11Mit62+30	13–31	0.00894**	0.00374
QTL-SH11.2		D11Mit14	10	87	D11Mit15+6– D11Mit14+18	63–97	0.00403**	0.00527*
QTL-SH12.1	22.39**	D12Mit2	6	27	D12Mit2+0– D12Mit2+12	21–33	0.00635**	0.00292

(*continued*)

TABLE 3

(Continued)

QTL	LOD	Proximal marker	Marker distance	Centromere distance	Marker C.I.	Centromere C.I.	Additive magnitude ‖**a**‖	Dominance magnitude ‖**d**‖
QTL-SH12.2		D12Mit5	4	45	D12Mit2+8– D12Nds2+0^{end}	29–70	0.00420**	0.00294
QTL-SH13.1	3.40**	D13Mit9	28	91	D13Mit9+16– D13Mit35+0^{end}	79–97	0.00234**	0.00247
QTL-SH14.1	4.19**	D14Mit5	14	60	D14Mit5+2– D14Mit7+0^{end}	48–64	0.00310**	0.00136
QTL-SH15.1	4.64**	D15Mit5	10	39	D15Mit13+16– D15Mit5+24	29–53	0.00393**	0.00261
QTL-SH15.2		D15Mit42	0	85	D15Mit5+24– D15Mit42+0^{end}	53–85	0.00312**	0.00122
QTL-SH16.1	2.30*	D16Mit2	16	26	D16Mit2+0^{end}_ D16Mit5+0^{end}	14–44	0.00323**	0.00194
QTL-SH18.1	5.29**	D18Mit17	14	79	D18Mit12+0^{end}_ D18Mit17+26	61–91	0.00452**	0.00318
QTL-SH19.1	2.50*	D19Mit14	18	39	D19Mit16+0^{end}_ D19Mit14+40	15–61	0.00304**	0.00749
Signed asymmetry								
QTL-SS15.1	3.52**	D15Mit5	14	43	D15Mit13+6– D15Mit5+20	11–55	0.00388**	0.00231
Unsigned asymmetry								
QTL-SU12.1	2.16*	D12Mit5	8	49	D12Mit5+2– D12Mit6+12	43–63	0.00175*	0.00236

Tabled values are LOD scores, locations (as map distances from the nearest proximal marker and from the centromere), their confidence intervals (C.I.), and the magnitudes of additive and dominance effects. The superscript "end" denotes a confidence interval truncated at the position of an extreme marker (including *D2Mit17*).
*$P < 0.05$; **$P < 0.01$.
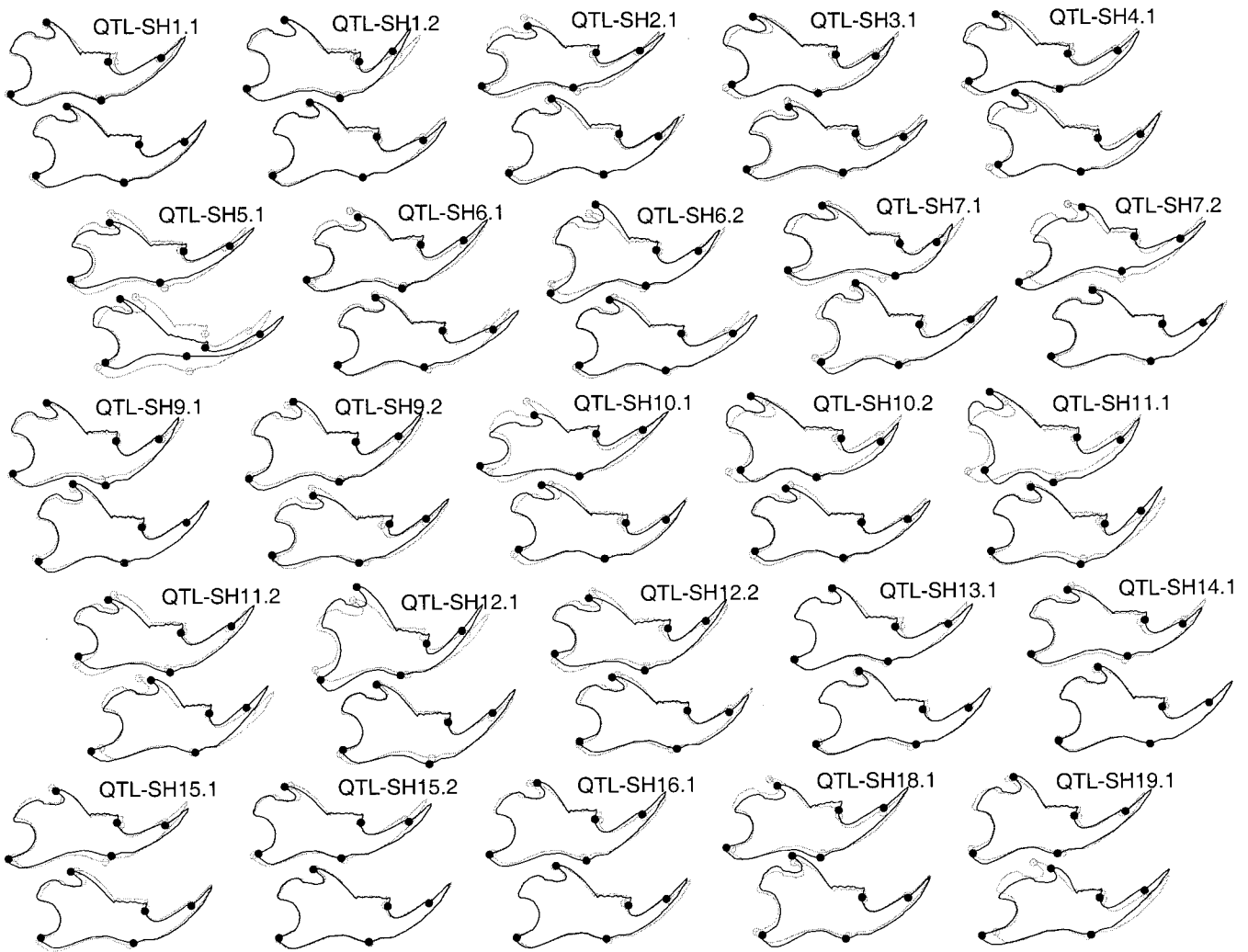
FIGURE 2.—QTL effects on shape (mean of left and right body sides). For each QTL, the additive effect is shown in the top diagram and the dominance effect below. In each diagram, the landmarks indicated by the open dots and gray outline represent the shape for the overall mean configuration, whereas the solid dots and black outline represent the mean shape with the respective QTL effect added—the QTL effect itself is the change between these two shapes. Because the QTL effects are subtle, all have been amplified by a factor of 25. Note that the outlines are drawn only to visualize the shape changes and that they are merely "pushed or pulled along" by the shifts of the landmarks themselves: changes in the outlines should therefore be interpreted with caution, especially where there are no landmarks (*e.g.*, in the condyle).

The spatial patterns of QTL effects concern the parts of the jaw that are affected and the directions of landmark shifts (Figure 2). Several patterns of change occur in a number of QTL, indicating that multiple loci affect similar shape features (Figure 2). One of these patterns is a relative shift of landmarks 1 and 5 in opposite directions along the antero-posterior axis, corresponding to shortening of the coronoid process and lengthening of the angular process, or vice versa. In many of these cases, there are only small changes in the positions of the other landmarks. This type of shape change can occur for either additive (*e.g.*, QTL-SH3.1, QTL-SH7.2) or dominance effects (*e.g.*, QTL-SH4.1, QTL-SH19.1). The fact that the shape changes can occur in either direction (*e.g.*, the additive effects of QTL-SH7.2 *vs.* QTL-SH10.2) indicates that these shape features are not

specifically associated with the SM/J or LG/J lines. A second recurrent pattern is relative movement of the same landmarks (1 and 5) toward or away from each other, that is, an opposite movement of the coronoid and angular processes that either expands or contracts the posterior part of the jaw in dorso-ventral direction. This pattern is seen, for instance, in the additive effects of QTL-SH11.2 and QTL-SH12.1 and the dominance effects of QTL-SH7.1 and QTL-SH10.2.

The dorso-ventral contraction and expansion is also found in the spatial patterns for the two QTL affecting shape asymmetry, although it is considerably weaker (Figure 3; additive effect of QTL-SS15.1 and dominance effect of QTL-SU12.1).

Multivariate distribution of QTL effects: In the ordinations of QTL effects by principal component analysis,
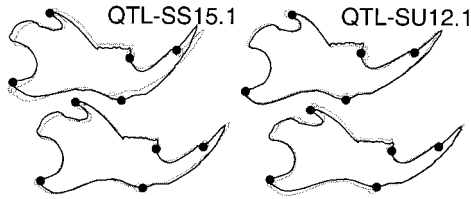
FIGURE 3.—QTL effects on signed (SS) and unsigned (SU) asymmetry of shape. For explanation of the diagrams, see Figure 2.

the same two patterns of variation also reappear as the first and second principal components (PCs) in separate analyses of the additive and dominance effects of the 25 QTL (Figure 4). In both analyses, the PC1s are associated with opposite anterior-posterior shifts of the angular and coronoid processes, and the PC2s are associated with dorso-ventral expansion or contraction. The PC1 and PC2 together account for 71.5% of the total variance for **a** vectors and 69.1% for the **d** vectors. Most of the variation in shape effects among QTL is therefore concentrated in two of the six available dimensions.

The scatter of **a** and **d** vectors around their means does not show any sign of clustering into distinct groups

of QTL in either analysis (Figure 4). The tests for the partitioning of QTL into either two or three groups by k-means clustering did not provide evidence for it either: the null hypothesis of a homogeneous distribution could be rejected neither for the additive effects ($g = 2$: ratio of within-cluster to total sum of squares 0.716, $P = 0.92$; $g = 3$: ratio 0.556, $P = 0.92$) nor for the dominance effects ($g = 2$: ratio 0.724, $P = 0.97$; $g = 3$: ratio 0.542, $P = 0.82$). Overall, therefore, variation appears to be continuous, and there is no evidence for distinct groups of QTL according to their effects on mandible shape. The two main patterns (corresponding to the PC1 and PC2) contribute to the additive and dominance effects of individual QTL to variable extents and in variable combinations.

Additive and dominance effects on shape: The additive and dominance effects of each QTL tend to differ from each other and do not appear to affect the same features of shape variation (Figure 2). The permutation test did not reject the null hypothesis of independence between additive and dominance effects (sum of squared covariances = 1.14×10^{-8}; $P = 0.074$). This result does not imply that there is no relationship at all between additive and dominance effects at each QTL,
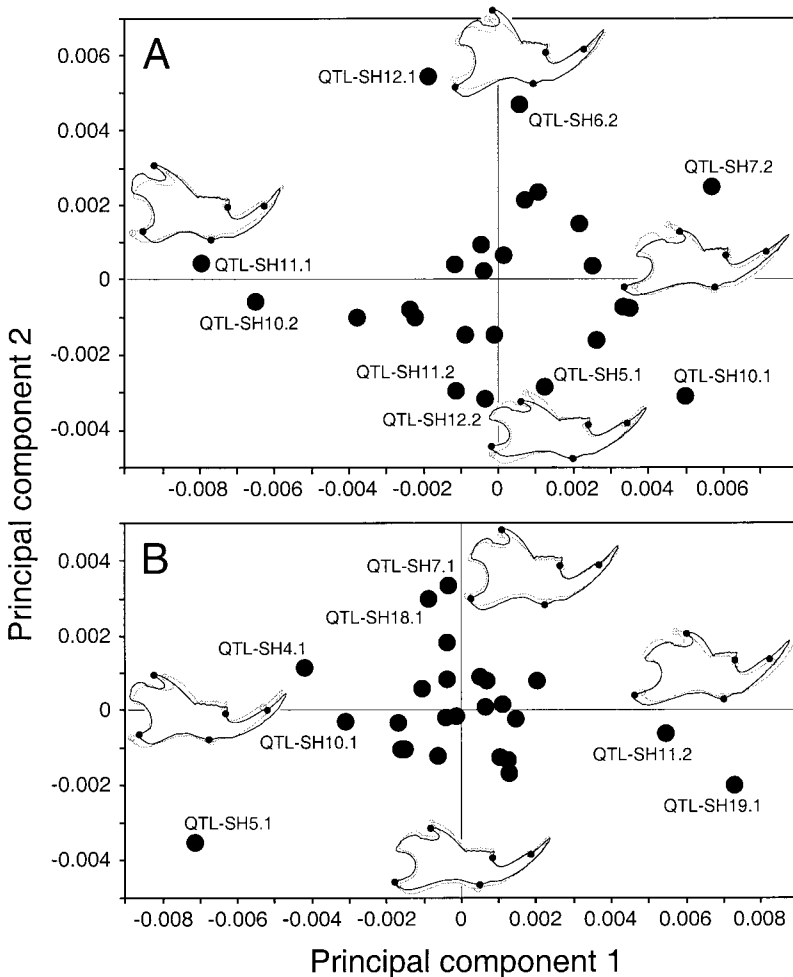
FIGURE 4.—Principal component analysis of QTL effects on shape. (A) Additive effects. (B) Dominance effects. The diagrams of mandibles drawn on the PC axes represent the shape changes corresponding to the PCs: they are configurations corresponding to the mean (open dots and gray outline) plus/minus two standard deviations for the respective PC (solid dots, black outlines). These effects are amplified by a factor of 25 as in Figure 2.

because there is a high degree of statistical uncertainty (recall that many of the dominance effects were not statistically significant). It clearly does indicate, however, that additive and dominance effects of a given QTL are not tightly associated, but tend to occupy different dimensions of shape space.

DISCUSSION

We have introduced new multivariate techniques to study the genetic architecture of size and shape. Our approach differs from previous ones in that it considers shape as a single multidimensional property of a morphological structure like the mouse mandible. Rather than extracting a series of scalar traits from the overall shape and performing univariate analyses on each of them separately, our approach is based on a single multivariate analysis of the entire shape information. While our results are generally consistent with previous analyses of this data set, we emphasize a number of new possibilities for further studies.

Comparison with previous studies: Our study has located 12 QTL affecting centroid size and 25 QTL affecting shape. This is similar to the putative 34 QTL for distance measurements identified by LEAMY *et al.* (1997, Appendix) and the 37 QTL listed by CHEVERUD *et al.* (1997; in addition, they reported four unnamed loci affecting a single distance each). Note, however, that these numbers of QTL are difficult to compare. On the one hand, 9 of the QTL for shape lie within or adjoin the confidence interval of a QTL for centroid size (Tables 2 and 3), which raises the possibility that these may be single loci with joint effects on both size and shape (a minimum estimate would thus be a total of 28 QTL). On the other hand, the previous studies had to combine QTL from separate analyses of interlandmark distances, exacerbating the problems with multiple testing that are inherent in QTL mapping. Unfortunately, these difficulties preclude a direct comparison of statistical power between the two approaches (but see CHEVERUD 2000).

The confidence intervals of all 12 QTL for centroid size contain at least 1 QTL identified in each of the previous analyses, and the majority of the 25 QTL for shape also have direct counterparts in the previous studies (20 in Leamy *et al.* and 21 in Cheverud *et al.*; see Table 4). The QTL for size appear to have more general effects than the QTL for shape. The counterparts of our size QTL in the study of LEAMY *et al.* (1997) affect an average of 5.5 interlandmark distances and 9 of the 12 involve all five landmarks, while the counterparts of the QTL for shape affect 3.95 distance traits on average, and only half of these involve all five landmarks. Likewise, in the study of CHEVERUD *et al.* (1997), 4 of the 14 QTL that were counterparts to our size QTL were classified as affecting the whole mandible, whereas only 3 of 23 counterparts to our shape QTL were so classified

(this comparison excludes those QTL that could not be classified; *cf.* Table 4). Although all these comparisons must remain informal, they suggest that the results of our study and the previous ones agree in considerable detail.

The predominance of QTL with effects on shape is also consistent with an earlier analysis: only 6 of the 26 classified QTL affected distance measurements throughout the whole mandible whereas the effects of the other 20 QTL were confined to specific regions (CHEVERUD *et al.* 1997). Perhaps the relatively simple genetic basis of size reflects the developmental control of size and its coordination through endocrine mechanisms (*e.g.*, SHEA 1992; BÜNGER and HILL 1999). It is possible, however, that the diversity of genetic controls for shape is simply a consequence of the sheer complexity of composite structures. The mouse mandible develops from several cell populations of distinct embryonic origins, which engage in an elaborate sequence of interactions, from early patterning events to bone remodeling extending long into the postnatal period (ATCHLEY and HALL 1991; HERRING 1993; FRANCIS-WEST *et al.* 1998). This complex makeup provides numerous degrees of freedom for variation in the proportions and arrangement of parts, and any gene participating in these processes has the potential to affect final shape.

Shape effects of QTL: Although the QTL effects on mandible shape are diverse, our analysis has identified two features of shape variation recurring in the effects of many QTL (Figures 2 and 3). They correspond to shifts of the positions of the coronoid and angular processes (landmarks 1 and 5) relative to each other and to the rest of the mandible in anterior-posterior and in dorso-ventral directions, respectively. The same patterns also appear in the first two PCs in separate analyses of additive and dominance effects (Figure 4), which in each analysis account for more than two-thirds of the total variance among QTL. The concentration of QTL effects on these two landmarks is consistent with an earlier study reporting that fully half of the QTL for distances between landmarks had effects that were confined exclusively to the ascending ramus of the mandible (CHEVERUD *et al.* 1997).

These patterns of shape variation have a counterpart, although in a much more extreme form, in the phenotypes produced by knockout experiments for several of the genes involved in craniofacial development (reviewed by FRANCIS-WEST *et al.* 1998). For instance, the angular and coronoid processes of the mandible are both severely reduced in gene knockouts for *goosecoid* (see Figure 5B; RIVERA-PÉREZ *et al.* 1995; YAMADA *et al.* 1995). Comparison of the mandible outlines of wild-type and *goosecoid* knockout mice (Figure 5, A *vs.* B) shows that the tips of the angular and coronoid processes both move in an anterior direction and toward each other in dorsal-ventral directions. If both the wild-type and the (smaller) knockout mandible are scaled

<div align="center">

TABLE 4

Comparison with the results of two previous QTL analyses of mandible morphology in the same mice

</div>

| | | Leamy *et al.* (1997) | | | | | | Cheverud *et al.* (1997) | |
| | | Landmarks affected | | | | | | | |
QTL	No. of QTL	1	2	3	4	5	Distances affected	Names of QTL	Subregions affected
Centroid size									
QTL-C2.1	1		•	•	•	•	4	QTMAN2-2	Ascending
QTL-C3.1	2	•	•	•	•	•	7	QTMAN3-2	Coronoid
QTL-C4.1	1	•	•	•	•	•	6	QTMAN4-1	Ascending
QTL-C6.1	1	•	•	•	•	•	8	QTMAN6-2	Molar
QTL-C7.1	2	•	•	•	•	•	5	QTMAN7-1, QTMAN7-2	
QTL-C10.1	1	•	•	•	•	•	7	QTMAN10-2	Condylar
QTL-C11.1	1	•	•		•		2	QTMAN11-2	Total
QTL-C11.2	1		•	•	•	•	3	QTMAN11-3, QTMAN11-4	Total, Molar
QTL-C13.1	1	•	•	•	•	•	8	QTMAN13-1	Coronoid
QTL-C14.1	1	•	•	•	•	•	7	QTMAN14-1, QTMAN14-2	Total, Total
QTL-C15.1	1	•	•	•	•	•	3	QTMAN15-1, QTMAN15-2	Molar, Condylar
QTL-C17.1	1	•	•	•	•	•	6	QTMAN17-1	Molar
Shape									
QTL-SH1.1	2	•	•	•	•	•	5	QTMAN1-1	Condylar
QTL-SH1.2	1	•	•	•	•	•	6	Unnamed	molar
QTL-SH2.1	0							QTMAN2-2	Ascending
QTL-SH3.1	1	•	•	•	•	•	7	QTMAN3-2	Coronoid
QTL-SH4.1	1	•	•	•	•	•	6	QTMAN4-1	Ascending
QTL-SH5.1	1			•	•		1	Unnamed	coronoid
QTL-SH6.1	1		•		•		1	QTMAN6-1	Molar
QTL-SH6.2	1	•	•	•	•	•	8	QTMAN6-2	Molar
QTL-SH7.1	1	•	•	•	•	•	4	QTMAN7-1	
QTL-SH7.2	1		•	•	•	•	3		
QTL-SH9.1	0							QTMAN9-1	Condylar
QTL-SH9.2	0								
QTL-SH10.1	1		•	•	•	•	3	QTMAN10-1	Molar
QTL-SH10.2	1	•	•	•	•	•	7		
QTL-SH11.1	0							QTMAN11-1	Ascending
QTL-SH11.2	1		•	•	•	•	3	QTMAN11-3	Total
QTL-SH12.1	0								
QTL-SH12.2	2	•	•	•	•		3	QTMAN12-2, QTMAN12-3	Incisor, Alveolar
QTL-SH13.1	1		•	•	•	•	2	QTMAN13-2	Incisor
QTL-SH14.1	1	•	•	•	•	•	7	QTMAN14-2	Total
QTL-SH15.1	1	•	•	•	•	•	3	QTMAN15-1	Molar
QTL-SH15.2	1	•	•	•			2	QTMAN15-2, QTMAN15-3	Condylar, Coronoid
QTL-SH16.1	1		•	•		•	2	QTMAN16-1	Total
QTL-SH18.1	1	•	•		•		2	QTMAN18-1	Ascending
QTL-SH19.1	2	•	•	•	•		4	QTMAN19-1	Coronoid, Masseteric

The table lists the QTL from previous studies that lie within the confidence intervals for all QTL for centroid size and shape identified by our analyses (Tables 2 and 3). For the QTL from Leamy *et al.* (1997, Appendix), the table indicates the number of QTL contained in the respective confidence interval, all the landmarks that define the distances affected by those QTL (*cf.* Figure 1), and the number of distances affected. For the QTL from Cheverud *et al.* (1997), the table names the QTL and lists the subregions of the mandible they affect (subregions are capitalized for the QTL classified as in the original study, but are in lowercase for QTL affecting only single distances, which were not named and classified by Cheverud *et al.*). We included a QTL from a previous study if its location, or at least some of its range, was within the confidence interval of a QTL estimated in the present study, but not if it was located exactly at the boundary of the confidence interval.

to the same overall size, the remaining difference is a net shape change where the coronoid and angular processes move toward each other primarily in dorsal-ventral direction, just as we found it in a more subtle way for several QTL (Figures 2 and 3) and the PC2s of the QTL effects (Figure 4). Moreover, a study of mouse chimeras composed of wild-type and *goosecoid* knockout cells showed that the severity of the reduction of angular
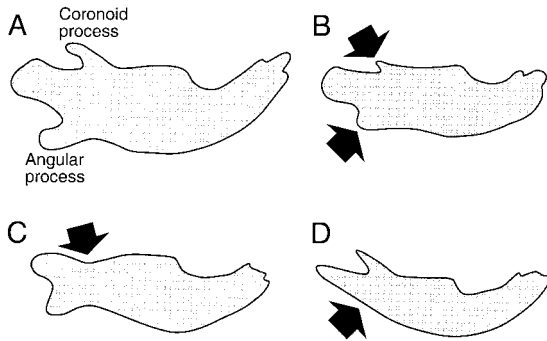
Figure 5.—Phenotypic effects of gene knockouts on mouse mandibles. Arrows indicate the main changes of the angular and coronoid processes. (A) Wild type. (B) Homozygous *goosecoid* deficiency (redrawn from Yamada *et al.* 1995). (C) Homozygous *Dlx5* deficiency (redrawn from Depew *et al.* 1999). (D) Homozygous TGFβ2 deficiency (redrawn from Sanford *et al.* 1997). The outlines in A–C are newborn mice, whereas D is at stage E18.5. The outlines are drawn roughly to scale (according to the mandibles of wild-type littermates of knockout mice depicted in the publications).

and coronoid processes is dose dependent (Rivera-Pérez *et al.* 1999), suggesting that the same developmental processes may affect the mandibular phenotype to different degrees depending on the level of gene activity. *goosecoid* is a possible candidate gene for QTL-SH12.2, because its position (on chromosome 12 at 52.0 cM centromere distance; Mouse Genome Database 2000) is close to the estimated QTL location and well within the confidence interval. Nevertheless, the statistical uncertainty of the estimated QTL position makes it impossible to conclude with confidence that the observed effects are related to this specific gene.

Similar reductions of both the angular and coronoid processes have been reported from double mutants of *Gli2* and *Gli3* (Mo *et al.* 1997) and, along with other severe mandibular defects, in knockouts for *Prx-1* and *Prx-2* (ten Berge *et al.* 1998; Lu *et al.* 1999a) and *Ptx1* (Lanctôt *et al.* 1999). Of these genes, only one is within the confidence intervals of any of the QTL in our study: *Prx-1* (synonym Pmx1, on chromosome 1 at 85.4 cM centromere distance, or marker D1Mit14+4 cM; Mouse Genome Database 2000), which is located near QTL-SH1.2. However, neither the additive nor dominance effect of this QTL has a geometric pattern that resembles the knockout effects, which makes this gene less likely as a candidate for the QTL.

The other recurring pattern of shape variation is a movement of the angular and coronoid processes in opposite anterior-posterior directions (Figure 2 and the PC1 in Figure 4). This pattern can be related to the phenotypic effects of gene knockouts where either the angular or coronoid processes are severely reduced, such as *Dlx5* (Figure 5C; Acampora *et al.* 1999; Depew *et al.* 1999) and TGFβ2 (Figure 5D; Sanford *et al.* 1997). If the configuration of landmarks from a *Dlx5* mutant

mandible with reduced coronoid process is scaled to the same size as that of the wild-type mandible, the tip of the coronoid process will be more anterior than in the wild-type configuration, but the less affected angular process will protrude posteriorly beyond the wild-type configuration, producing an apparent movement of both those landmarks against each other in anterior-posterior direction. The reverse applies for the TGFβ2 mutant phenotype. Thus independent variation of either the angular or coronoid processes can account for their anterior-posterior shifts relative to one another. *Dlx5* (on chromosome 6 at 2.0 cM centromere distance; Mouse Genome Database 2000) is a potential candidate gene for QTL-SH6.1, which shows this pattern in its additive effect, but as above, this assignment must remain tentative because of the statistical uncertainty of QTL mapping. Although TGFβ2 is fairly close to QTL-SH1.2 (on chromosome 1 at 101.5 cM centromere distance or marker D1Mit14+14 cM; Mouse Genome Database 2000), the inconsistency between the geometric patterns of QTL effects and knockout phenotype suggests that it is not a likely candidate gene.

Relating the geometric patterns of QTL effects to phenotypic changes caused by gene knockouts can provide a new piece of evidence in the search for candidate genes. However, because confidence intervals of QTL extend over sizeable chromosome regions that include many genes, the support provided by the agreement of patterns should be interpreted with caution. Perhaps it is better to think of this evidence as an additional test for the hypothesis that a particular gene is a candidate for a QTL: inconsistency of QTL and knockout patterns, then, is evidence against that hypothesis. However, because different alleles (and combinations of alleles) can have different effects, and because epistatic interactions lead to a dependence on the genetic background, the geometric patterns can neither implicate nor rule out a gene conclusively. Increasing the spatial resolution of the morphometric analysis by including additional landmarks will make the patterns of QTL effect a more decisive test of candidate gene hypotheses and can complement improvements in the resolution of linkage mapping by increasing sample size and marker density.

Gene functions and QTL for asymmetry: Although only one QTL for asymmetry was well supported statistically, the presence of QTL for asymmetry has been shown in previous studies (Leamy *et al.* 1997, 1998). This raises the question whether they also can be related to the results from knockout studies. An interesting case of a gene that may provide insight into the genetic basis of morphological asymmetry is *Pitx2*, because it functions both in craniofacial development and in generating the large difference between left and right lungs (Gage *et al.* 1999; Lin *et al.* 1999; Lu *et al.* 1999b). While participation of the same genes in both processes is not a necessary condition, it underscores the multiple connections between developmental pathways with widely

different functions. Accordingly, at least in principle, these pathways can be responsive to diverse inputs of positional information, such as left-right differences. Mice heterozygous for a *Pitx2* null allele show, among other defects, malocclusion of teeth in conjunction with marked asymmetry of the incisors (Gage *et al.* 1999, Figure 3E). The effects of this null mutation are thus (partially) dominant, just as in humans, where loss of one copy of the gene causes a haploinsufficiency condition, Rieger's syndrome (Lu *et al.* 1999b). The role of nonadditive variation for the genetic basis of fluctuating asymmetry is also underscored by theoretical modeling of developmental processes (Klingenberg and Nijhout 1999; Klingenberg 2001) and empirical evidence from QTL studies (Leamy 2001). While these results may be suggestive, it is clear that the mechanisms that constitute the genetic basis of morphological asymmetry require further study.

Multivariate distribution of QTL effects: Recent theories on the evolution of genetic architecture, based on the concept of morphological integration (Olson and Miller 1958), predict that pleiotropic effects of genes should coincide with the developmental and functional relationships between structures (Cheverud 1984, 1996; Wagner and Altenberg 1996). Multivariate analyses of the distribution of QTL effects are a new source of information, complementing studies examining the spatial domains of QTL effects (Cheverud *et al.* 1997; Leamy *et al.* 1999; Mezey *et al.* 2000) as an additional test of these theories.

If the pleiotropic effects of genes reflect functional relationships of traits, then their phenotypic effects should form distinct clusters according to function. Cheverud *et al.* (1997) reported that 50% of the QTL had effects that were restricted to the ascending ramus of the mandible and 27% affected only the alveolar region, whereas 23% had significant effects in both regions (see also Mezey *et al.* 2000). Accordingly, two clusters of QTL would be expected, one affecting the alveolar process and the other the ascending ramus, and perhaps a third cluster with QTL affecting the entire mandible. However, the variation of shape effects among QTL shows no evidence of such clustering into distinct groups, either from the scatter of PC scores (Figure 4) or from the test for two or three clusters in the data.

Instead of distinct classes of QTL, the scatter along the first two PC axes suggests continuous variation in the degree to which the effects of each QTL corresponded to the two main patterns of shape variation. At first, this lack of clustering of multivariate QTL effects may seem at odds with the previous findings of a clear distinction of QTL affecting different parts of the mandible. Even within those groups, however, QTL affect interlandmark distances in various combinations (Cheverud *et al.* 1997, Figure 4), and therefore the groups do not appear to form monolithic classes. Our multivariate

shape analysis has emphasized the complex nature of variation among QTL, which needs to be further investigated in more extensive studies using multivariate methods.

The expectation from theory is that functionally independent parts should vary independently among QTL and therefore should be associated with different PCs. In this study, the dominant PCs are associated entirely with variation of the angular and coronoid processes, which are part of a single functional complex serving for attachment of the masticatory musculature (*e.g.*, Atchley and Hall 1991). Because only one functional complex is involved, the PCs of QTL effects do not provide decisive information with regard to hypotheses on integration. Denser coverage of the mandible with additional landmarks would likely produce a much more differentiated picture of morphological integration in QTL effects. For instance, a study considering 17 landmarks has shown that patterns of phenotypic variation in shrew mandibles reflect the insertion of individual muscles (Badyaev and Foresman 2000).

Additive and dominance effects: For centroid size, the estimates of dominance effects are substantially smaller than the corresponding additive effects, whereas for shape, the dominance effects are nearly as large, on average, as the additive effects of the same QTL (*cf.* Tables 2 and 3). For 6 of the 25 shape QTL, dominance effects even were greater than the additive effects. That the dominance effects on shape were statistically significant for only 6 QTL, however, may be surprising given their magnitudes and is a reminder of the limited statistical power for detecting dominance. It is therefore necessary to interpret the results with some caution.

If localized expression and developmental functions of genes are causing the geometric patterns of QTL effects, then one would expect that the additive and dominance effects of each QTL should have similar spatial patterns. For most QTL, however, the additive and dominance effects on shape are markedly different (Figure 2) and can even affect entirely separate parts of the mandible (*e.g.*, QTL-SH11.1). The permutation test did not show a statistically significant association between additive and dominance effects, although the P value of 0.07 may still be taken as evidence, albeit weak, against the null hypothesis of total independence. It is clear, however, that the vectors of additive and dominance effects of each QTL are not collinear; that is, they tend to point in different directions of shape space.

Dominance is measured as the difference between the genotypic values of the heterozygote and the average of the two homozygotes (*e.g.*, Falconer and Mackay 1996). In univariate studies, dominance necessarily implies that the heterozygote is more similar to one of the homozygotes than to the other (in the case of overdominance or underdominance, the heterozygote is more extreme than either homozygote). In the present multi-

variate context, however, genotypic values are not constrained to be arranged along a single line and so are free to vary in features located in orthogonal directions of shape space (*e.g.*, shifts of different landmarks or shifts in different directions). Thus the points representing the average shapes of the two homozygotes and the heterozygote can form a triangle in a multivariate shape space. Half the length of the baseline between the two homozygotes stands for the additive effect, and the line from the midpoint of this baseline to the heterozygote is the dominance effect. If the additive and dominance effects point in different directions, as in the present study, then the heterozygote will be at some distance from the baseline. The greater this distance from the baseline, the more the heterozygote will show shape features that neither homozygote has, and therefore it exhibits overdominance.

It is not clear what this sort of overdominance in a multidimensional context implies for the maintenance of genetic variation in populations under selection for shape. This depends on the magnitudes and directions of the vectors of additive and dominance effects. Theoretical studies of the consequences of this multivariate concept of genetic architecture on evolutionary dynamics are clearly warranted, and the multivariate distribution of additive and dominance effects needs to be further investigated empirically in this and other study systems.

Geometric morphometrics and QTL mapping: Overall, the results of our study using geometric morphometrics are consistent with those of QTL analyses of multiple interlandmark distances. However, geometric morphometrics makes it easy to present the output of statistical analyses in a graphical form that relates immediately to the morphological structures at hand. For instance, it makes possible a direct comparison of the geometric pattern of QTL effects to phenotypes produced by gene knockout experiments and thus provides additional evidence for evaluating the hypothesis that a particular gene is a candidate for a given QTL. More importantly, this method offers a new perspective because it treats shape as a single, but multidimensional, phenomenon (a corresponding treatment of morphology based on interlandmark distances is possible in principle, but rarely used). This allows the study of variation among QTL in terms of the multivariate distribution of their phenotypic effects and offers new tests, for instance, for theories of morphological integration. Moreover, if additive and dominance effects are considered as vectors in a multidimensional shape space, it follows that overdominance in certain features of shape is normally to be expected, possibly with important implications for the maintenance of variation in populations under selection. The use of geometric morphometrics in the context of QTL analyses therefore provides new possibilities for studies at the interface of evolutionary and developmental genetics.

LITERATURE CITED

Acampora, D., G. R. Merlo, L. Paleari, B. Zerega, M. P. Postiglione *et al.*, 1999 Craniofacial, vestibular and bone defects in mice lacking the *Distal-less* related gene *Dlx5*. Development **126:** 3795–3809.

Atchley, W. R., and B. K. Hall, 1991 A model for development and evolution of complex morphological structures. Biol. Rev. **66:** 101–157.

Auffray, J.-C., V. Debat and P. Alibert, 1999 Shape asymmetry and developmental stability, pp. 309–324 in *On Growth and Form: Spatio-Temporal Pattern Formation in Biology*, edited by M. A. J. Chaplain, G. D. Singh and J. C. McLachlan. Wiley, Chichester, UK.

Badyaev, A. V., and K. R. Foresman, 2000 Extreme environmental change and evolution: stress-induced morphological variation is strongly concordant with patterns of evolutionary divergence in shrew mandibles. Proc. R. Soc. Lond. Ser. B Biol. Sci. **267:** 371–377.

Bailey, D. W., 1985 Genes that affect the shape of the murine mandible: congenic strain analysis. J. Hered. **76:** 107–114.

Bailey, D. W., 1986 Genes that affect morphogenesis of the murine mandible: recombinant-inbred strain analysis. J. Hered. **77:** 17–25.

Birdsall, K., E. Zimmerman, K. Teeter and G. Gibson, 2000 Genetic variation for the positioning of wing veins in *Drosophila melanogaster*. Evol. Dev. **2:** 16–24.

Bookstein, F. L., 1991 *Morphometric Tools for Landmark Data: Geometry and Biology*. Cambridge University Press, Cambridge, UK.

Bookstein, F. L., 1996a Biometrics, biomathematics and the morphometric synthesis. Bull. Math. Biol. **58:** 313–365.

Bookstein, F. L., 1996b Combining the tools of geometric morphometrics, pp. 131–151 in *Advances in Morphometrics*, edited by L. F. Marcus, M. Corti, A. Loy, G. J. P. Naylor and D. E. Slice. Plenum Press, New York.

Bünger, L., and W. G. Hill, 1999 Role of growth hormone in the genetic change of mice divergently selected for body weight and fatness. Genet. Res. **74:** 351–360.

Cavicchi, S., G. Giorgi, V. Natali and D. Guerra, 1991 Temperature-related divergence in experimental populations of *Drosophila melanogaster*. III. Fourier and centroid analysis of wing shape and relationship between shape variation and fitness. J. Evol. Biol. **4:** 141–159.

Chai, C., 1956 Analysis of quantitative inheritance of body size in mice. I. Hybridization and maternal influence. Genetics **41:** 157–164.

Cheverud, J. M., 1984 Quantitative genetics and developmental constraints on evolution by selection. J. Theor. Biol. **110:** 155–171.

Cheverud, J. M., 1996 Developmental integration and the evolution of pleiotropy. Am. Zool. **36:** 44–50.

Cheverud, J. M., 2000 The genetic architecture of pleiotropic relations and differential epistasis, pp. 411–433 in *The Character Concept in Evolutionary Biology*, edited by G. P. Wagner. Academic Press, San Diego.

Cheverud, J. M., S. E. Hartman, J. T. Richtsmeier and W. R. Atchley, 1991 A quantitative genetic analysis of localized morphology in mandibles of inbred mice using finite element scaling. J. Craniofacial Genet. Dev. Biol. **11:** 122–137.

Cheverud, J. M., E. J. Routman, F. A. M. Duarte, B. van Swinderen, K. Cothran *et al.*, 1996 Quantitative trait loci for murine growth. Genetics **142:** 1305–1319.

Cheverud, J. M., E. J. Routman and D. J. Irschick, 1997 Pleiotropic effects of individual gene loci on mandibular morphology. Evolution **51:** 2006–2016.

CHURCHILL, G. A., and R. W. DOERGE, 1994 Empirical threshold values for quantitative trait mapping. Genetics **138:** 963–971.

DEBAT, V., P. ALIBERT, P. DAVID, E. PARADIS and J.-C. AUFFRAY, 2000 Independence between developmental stability and canalization in the skull of the house mouse. Proc. R. Soc. Lond. Ser. B Biol. Sci. **267:** 423–430.

DEPEW, M. J., J. K. LIU, J. E. LONG, R. PRESLEY, J. J. MENESES *et al.*, 1999 *Dlx5* regulates regional development of the branchial arches and sensory capsules. Development **126:** 3831–3846.

DRYDEN, I. L., and K. V. MARDIA, 1998 *Statistical Analysis of Shape.* Wiley, Chichester, UK.

EDGINGTON, E. S., 1995 *Randomization Tests.* Dekker, New York.

EFRON, B., and R. J. TIBSHIRANI, 1993 *An Introduction to the Bootstrap.* Chapman & Hall, New York.

FALCONER, D. S., and T. F. C. MACKAY, 1996 *Introduction to Quantitative Genetics.* Longman, Essex, UK.

FRANCIS-WEST, P., R. LADHER, A. BARLOW and A. GRAVESON, 1998 Signalling interactions during facial development. Mech. Dev. **75:** 3–28.

GAGE, P. J., H. SUH and S. A. CAMPER, 1999 Dosage requirement of *Pitx2* for development of multiple organs. Development **126:** 4643–4651.

GILCHRIST, A. S., R. B. R. AZEVEDO, L. PARTRIDGE and P. O'HIGGINS, 2000 Adaptation and constraint in the evolution of *Drosophila melanogster* wing shape. Evol. Dev. **2:** 114–124.

GOODALE, H., 1941 Progress report on possibilities in progeny test breeding. Science **94:** 442–443.

GREEN, 1978 *Analyzing Multivariate Data.* Dryden, Hinsdale, IL.

HALEY, C. S., and S. A. KNOTT, 1992 A simple regression method for mapping quantitative trait loci in line crosses using flanking markers. Heredity **69:** 315–324.

HALL, B. K., 1999 *Evolutionary Developmental Biology.* Kluwer, Dordrecht, The Netherlands.

HERRING, S. W., 1993 Formation of the vertebrate face: epigenetic and functional influences. Am. Zool. **33:** 472–483.

JANSEN, R. C., 1993 Interval mapping of multiple quantitative trait loci. Genetics **135:** 205–211.

JOLLIFFE, I. T., 1986 *Principal Component Analysis.* Springer-Verlag, New York.

KLINGENBERG, C. P., 2001 A developmental perspective on developmental instability: theory, models and mechanisms, in *Developmental Instability: Causes and Consequences*, edited by M. POLAK. Oxford University Press, New York (in press).

KLINGENBERG, C. P., and G. S. MCINTYRE, 1998 Geometric morphometrics of developmental instability: analyzing patterns of fluctuating asymmetry with Procrustes methods. Evolution **52:** 1363–1375.

KLINGENBERG, C. P., and H. F. NIJHOUT, 1999 Genetics of fluctuating asymmetry: a developmental model of developmental instability. Evolution **53:** 358–375.

KLINGENBERG, C. P., and S. D. ZAKLAN, 2000 Morphological integration between developmental compartments in the *Drosophila* wing. Evolution **54:** 1273–1285.

KÖNTGES, G., and A. LUMSDEN, 1996 Rhombencephalic neural crest segmentation is preserved throughout craniofacial ontogeny. Development **122:** 3229–3242.

KRZANOWSKI, W. J., and F. H. C. MARRIOTT, 1995 *Multivariate Analysis. Part 2. Classification, Covariance Structures and Repeated Measurements.* Arnold, London.

LANCTÔT, C., A. MOREAU, M. CHAMBERLAND, M. L. TREMBLAY and J. DROUIN, 1999 Hindlimb patterning and mandible development require the *Ptx1* gene. Development **126:** 1805–1810.

LANDER, E. S., P. GREEN, J. ABRAHAMSON, A. BARLOW, M. DALEY *et al.*, 1987 MAPMAKER: an interactive computer package for constructing primary genetic linkage maps of experimental and natural populations. Genomics **1:** 174–181.

LAURIE, C. C., J. R. TRUE, J. LIU and J. M. MERCER, 1997 An introgression analysis of quantitative trait loci that contribute to a morphological difference between *Drosophila simulans* and *D. mauritiana.* Genetics **145:** 339–348.

LEAMY, L., 1984 Morphometric studies in inbred and hybrid house mice. V. Directional and fluctuating asymmetry. Am. Nat. **123:** 579–593.

LEAMY, L. J., 2001 Dominance, epistasis, and fluctuating asymmetry, in *Developmental Instability: Causes and Consequences*, edited by M. POLAK. Oxford University Press, New York (in press).

LEAMY, L. J., E. J. ROUTMAN and J. M. CHEVERUD, 1997 A search for quantitative trait loci affecting asymmetry of mandibular characters in mice. Evolution **51:** 957–969.

LEAMY, L. J., E. J. ROUTMAN and J. M. CHEVERUD, 1998 Quantitative trait loci for fluctuating asymmetry of discrete skeletal characters in mice. Heredity **80:** 509–518.

LEAMY, L. J., E. J. ROUTMAN and J. M. CHEVERUD, 1999 Quantitative trait loci for early- and late-developing skull characters in mice: a test of the genetic independence model of morphological integration. Am. Nat. **153:** 201–214.

LEAMY, L. J., D. POMP, E. J. EISEN and J. M. CHEVERUD, 2000 Quantitative trait loci for directional but not fluctuating asymmetry of mandible characters in mice. Genet. Res. **76:** 27–40.

LIN, C. R., C. KIOUSSI, S. O'CONNELL, P. BRIATA, D. SZETO *et al.*, 1999 Pitx2 regulates lung asymmetry, cardiac positioning and pituitary and tooth morphogenesis. Nature **401:** 279–282.

LINCOLN, S., M. DALY and E. LANDER, 1992 *Constructing Genetic Maps with MAPMAKER/EXP 3.0*, Technical Report. Whitehead Institute, Cambridge, MA.

LIU, J., J. M. MERCER, L. F. STAM, G. C. GIBSON, Z-B. ZENG *et al.*, 1996 Genetic analysis of amorphological shape difference in the male genitalia of *Drosophila simulans* and *D. mauritiana.* Genetics **142:** 1129–1145.

LU, M.-F., H.-T. CHENG, M. J. KERN, S. S. POTTER, B. TRAN *et al.*, 1999a *prx-1* functions cooperatively with another *paired*-related homeobox gene, *prx-2*, to maintain cell fates within the craniofacial mesenchyme. Development **126:** 495–504.

LU, M.-F., C. PRESSMAN, R. DYER, R. L. JOHNSON and J. F. MARTIN, 1999b Function of Rieger syndrome gene in left–right asymmetry and craniofacial development. Nature **401:** 276–278.

LYNCH, M., and B. WALSH, 1998 *Genetics and Analysis of Quantitative Traits.* Sinauer, Sunderland, MA.

MACARTHUR, J., 1944 Genetics of body size and related characters. I. Selection of small and large races of the laboratory mouse. Am. Nat. **78:** 142–157.

MEZEY, J. G., J. M. CHEVERUD and G. P. WAGNER, 2000 Is the genotype-phenotype map modular? A statistical approach using mouse quantitative trait loci data. Genetics **156:** 305–311.

MO, R., A. M. FREER, D. L. ZINYK, M. A. CRACKOWER, J. MICHAUD *et al.*, 1997 Specific and redundant functions of *Gli2* and *Gli3* zinc finger genes in skeletal patterning and development. Development **124:** 113–123.

MOUSE GENOME DATABASE, 2000 Mouse Genome Informatics, Jackson Laboratory, Bar Harbor, ME, September 2000 (http://www.informatics.jax.org/).

OLSON, E. C., and R. L. MILLER, 1958 *Morphological Integration.* University of Chicago Press, Chicago.

PALMER, A. R., 1994 Fluctuating asymmetry analyses: a primer, pp. 335–364 in *Developmental Instability: Its Origins and Implications*, edited by T. A. MARKOW. Kluwer, Dordrecht, The Netherlands.

PALMER, A. R., and C. STROBECK, 1986 Fluctuating asymmetry: measurement, analysis, patterns. Annu. Rev. Ecol. Syst. **17:** 391–421.

RIVERA-PÉREZ, J. A., M. MALLO, M. GENDRON-MAGUIRE, T. GRIDLEY and R. R. BEHRINGER, 1995 *goosecoid* is not an essential component of the mouse gastrula organizer but is required for craniofacial and rib development. Development **121:** 3005–3012.

RIVERA-PÉREZ, J. A., M. WAKAMIYA and R. R. BEHRINGER, 1999 *Goosecoid* acts cell autonomously in mesenchyme-derived tissues during craniofacial development. Development **126:** 3811–3821.

ROUTMAN, E., and J. M. CHEVERUD, 1994 A rapid method of scoring simple sequence repeat polymorphism with agarose gel electrophoresis. Mamm. Genome **5:** 187–188.

ROUTMAN, E., and J. M. CHEVERUD, 1995 Polymorphism for PCR-analyzed microsatellites: data for two additional inbred mouse strains and the utility of agarose gel electrophoresis. Mamm. Genome **6:** 401–404.

SANFORD, L. P., I. ORMSBY, A. C. GITTENBERGER-DE GROOT, H. SARIOLA, R. FRIEDMAN *et al.*, 1997 TGFβ2 knockout mice have multiple developmental defects that are non-overlapping with other TGFβ knockout phenotypes. Development **124:** 2659–2670.

SHEA, B. T., 1992 Developmental perspective on size change and allometry in evolution. Evol. Anthropol. **1:** 125–134.

TEN BERGE, D., A. BROUWER, J. KORVING, J. F. MARTIN and F. MEIJLINK, 1998 *Prx1* and *Prx2* in skeletogenesis: roles in the craniofacial region, inner ear and limbs. Development **125:** 3831–3842.

WAGNER, G. P., and L. ALTENBERG, 1996   Complex adaptations and the evolution of evolvability. Evolution **50:** 967–976.

WEBER, K., R. EISMAN, L. MOREY, A. PATTY, J. SPARKS *et al.*, 1999   An analysis of polygenes affecting wing shape on chromosome 3 in *Drosophila melanogaster*. Genetics **153:** 773–786.

WEBER, K. E., 1990   Selection on wing allometry in *Drosophila melanogaster*. Genetics **126:** 975–989.

WEBER, K. E., 1992   How small are the smallest selectable domains of form? Genetics **130:** 345–353.

WHITLOCK, M. C., and K. FOWLER, 1999   The changes in genetic and environmental variance with inbreeding in *Drosophila melanogaster*. Genetics **152:** 345–353.

YAMADA, G., A. MANSOURI, M. TORRES, E. T. STUART, M. BLUM *et al.*, 1995   Targeted mutation of the murine *goosecoid* gene results in craniofacial defects and neonatal death. Development **121:** 2917–2922.

ZENG, Z-B., 1994   Precision mapping of quantitative trait loci. Genetics **136:** 1457–1465.

ZENG, Z-B., J. LIU, L. F. STAM, C.-H. KAO, J. M. MERCER *et al.*, 2000   Genetic architecture of a morphological shape difference between two Drosophila species. Genetics **154:** 299–310.

ZIMMERMAN, E., A. PALSSON and G. GIBSON, 2000   Quantitative trait loci affecting components of wing shape in *Drosophila melanogaster*. Genetics **155:** 671–683.